Available online at www.sciencedirect.com

ScienceDirect

Mendeleev Commun., 2018, **28**, 152–154

Mendeleev Communications

PdZn/α-Al_2O_3 catalyst for liquid-phase alkyne hydrogenation: effect of the solid-state alloy transformation into intermetallics

Igor S. Mashkovsky,*[a] Pavel V. Markov,[a] Galina O. Bragina,[a] Galina N. Baeva,[a] Aleksandr V. Rassolov,[a] Andrey V. Bukhtiyarov,[b] Igor P. Prosvirin,[b] Valery I. Bukhtiyarov[b] and Aleksandr Yu. Stakheev[a]

[a] *N. D. Zelinsky Institute of Organic Chemistry, Russian Academy of Sciences, 119991 Moscow, Russian Federation. Fax: +7 499 135 5328; e-mail: im@ioc.ac.ru*

[b] *G. K. Boreskov Institute of Catalysis, Siberian Branch of the Russian Academy of Sciences, 630090 Novosibirsk, Russian Federation*

DOI: 10.1016/j.mencom.2018.03.014

The complex characterization of a PdZn/Al_2O_3 catalyst by XPS, XRD, TEM and H_2-TPD techniques revealed the route of solid-state alloy → intermetallics transformation. The influence of this transformation on the performance of PdZn/Al_2O_3 in the liquid-phase hydrogenation of diphenylacetylene was estimated.

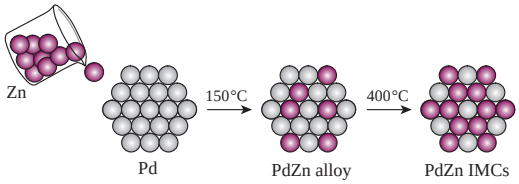

Nowadays, mono- and bimetallic clusters with controlled catalytic properties are extensively used as catalysts for a number of chemical processes due to the possibility of tuning their activity, selectivity and stability under reaction conditions.[1–6] Intermetallic compounds (IMCs) are of growing interest as highly selective heterogeneous catalysts.[7–9] In contrast to substituted alloys, IMCs are stable against segregation having ordered crystal structure different from the structure of the constituting metals. The intermetallic PdZn system is a promising catalytic composition, which is successfully used in industry for selective alkyne hydrogenation, methanol steam reforming, biomass conversion, *etc*.[10] Several reviews have been focused on the general properties of IMCs and on the properties of PdZn compositions in particular.[6,7,11] It is important that the PdZn system can form either substituted solid-state alloy or IMCs.[12] However, the effect of PdZn solid-state alloy–PdZn IMCs transformation on the catalytic performance was not studied in details. Here, to trace this effect, the PdZn/Al_2O_3 catalyst was reduced stepwise at 150, 200, 250, 300, 350 and 400 °C; after each reduction stage, a sample of the catalyst was taken for characterization and catalytic study. Details of catalyst preparation and characterization by XPS, XRD, TEM and H_2-TPD techniques can be found in Online Supplementary Materials.

The XPS study of the formation of Pd-Zn bimetallic particles was carried out by monitoring the Pd 3*d* and Zn 2*p* regions (Figure 1) after each step of catalyst reduction. Before reduction, Pd $3d_{5/2}$ and Zn $2p_{3/2}$ peaks were observed at 337.2 and 1022.3 eV for PdO and ZnO, respectively.[13,14] After reduction at 200–250 °C, the Pd $3d_{5/2}$ peak shifted to 335.8 eV indicating Pd^{2+} → Pd^0 reduction and characteristic of Pd^0 in PdZn alloy.[7,15,16] In the Zn 2*p* region, an additional signal appeared at 1020.5 eV characteristic of Zn^0. This observation suggests that the reduction of Zn is facilitated in the presence of Pd *via* hydrogen activated on Pd. Note that the Zn $2p_{3/2}$ binding energy is lower than that of metallic Zn (~1021.5 eV) denoting the formation of PdZn alloy.[12] XPS analysis also demonstrates that the Zn^0/Pd^0 ratio is about 1.0, and this value is achieved after reduction at 200 °C.

After reduction at 300 and 400 °C, Zn^0 $2p_{3/2}$ predominates indicating further reduction of Zn. Simultaneously, we can observe a minor shift of Pd $3d_{5/2}$ toward a lower binding energy by 0.3–0.4 eV. This shift can be tentatively ascribed to the formation of PdZn intermetallics (see XRD data below). Alternatively, it may be caused by Zn evaporation and partial depletion of the PdZn particle surface in zinc[17] since the Zn^0/Pd^0 ratio decreases from ~1.0 to ~0.5 after reduction at 400 °C.

Figure 2 shows XRD patterns for the PdZn/α-Al_2O_3 supported catalysts reduced at different temperatures. Profiles of Pd/α-Al_2O_3 and unreduced PdZn/α-Al_2O_3 are also displayed for comparison. For the reference monometallic Pd/Al_2O_3 catalyst, two XRD reflexes were observed at ~40.0° and ~46.7°, corresponding to Pd(111) and Pd(200), respectively.[18] The XRD pattern of the unreduced PdZn catalyst displays a group of signals at 31.0–35.0°. A wide and asymmetrical peak at ~34.0° can be attributed to PdO,[19] and low-intensity peaks at ~31.8°, ~34.3° and ~36.3° are assigned to (100), (002) and (101) of ZnO with a polycrystalline wurtzite structure, respectively.[20–22] No typical Zn^0 signals at 38.9°, 43.1° or 54.2° were observed.[14,23]

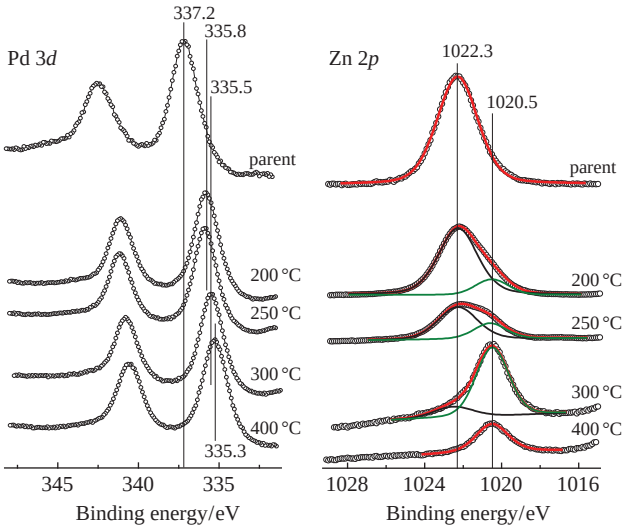

Figure 1 Pd 3*d* and Zn 2*p* XPS spectra of parent PdZn/α-Al_2O_3 catalysts and those reduced (H_2, 250 mbar, 1 h) at different temperatures.

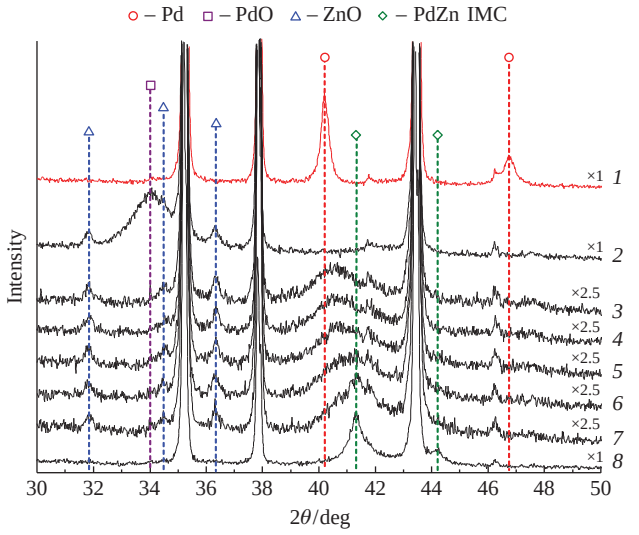

Figure 2 Comparison of XRD patterns for (*1*) Pd/α-Al_2O_3 and (*2*) PdZn/α-Al_2O_3 catalysts, parent and (*3*)–(*8*) reduced at (*3*) 150, (*4*) 200, (*5*) 250, (*6*) 300, (*7*) 350 and (*8*) 400 °C.

After PdZn/α-Al_2O_3 reduction at 150 °C, the intensities of PdO and ZnO signals diminished and a wide reflex appeared at ~39.0–41.5° Note that the position of its maximum does coincide with the position of Pd(111) ~ 40.0° in Pd/Al_2O_3 and is shifted toward higher 2θ with a maximum at 40.6°, which suggests the formation of PdZn substituted alloy even at a temperature of 150 °C. Low intensity of a signal, its asymmetry and the absence of the Pd(200) reflex at 46.7° indicate that the structure of the alloyed particles is largely disordered and the formed particles are small. These results are consistent with published data[24] and TEM data (Figure 3). The following H_2 treatment at 200 and 250 °C results in a gradual shift of the peak at 40.6° toward higher angles indicating the enrichment of PdZn solid solution in Zn.[25] Simultaneously, the intensity of ZnO reflex notably decreases.

The transformation of PdZn solid-state alloy to the intermetallic structure begins as the temperature is raised above 300 °C. A wide Bragg peak appears at ~41.4° ascribed to PdZn intermetallic compound.[9,22,26] However, the most part of PdZn particles is still as a solid-state alloy, as evidenced by the broadening and low intensity of a peak at ~41.4°. With a further increase in H_2 reduction temperature to 400°C, the intensity of this signal grows, and it becomes more symmetrical and intense. Moreover, an additional reflex appears at 44.0° giving distinct evidence for the formation of PdZn IMCs.[9,14] The asymmetry of this reflex indicates some irregularity of IMCs structure.[10,15,27]

Since our XPS and XRD data suggest the formation of PdZn alloy after reduction at 150–200 °C, we additionally verify its formation by an H_2-TPD method. A specific characteristic of Pd is its ability to absorb a considerable amount of H_2 to form α- and/or β-PdH_x hydride phases.[28,29] The hydrogen of this hydride structure is capable to migrate to Pd surface under reaction conditions enhancing the complete alkyne hydrogenation. However, upon the formation of a bimetallic PdM (M = Cu, Ag, In, Pb, *etc*.) alloy, the solubility of hydrogen significantly decreases; this makes it possible to avoid or minimize the PdH phase formation.[30,31] Thus, the higher selectivity of bimetallic or intermetallic hydrogenation catalysts can be attributed to the inhibition of palladium hydride phase formation.[8,32]

An H_2-TPD study was performed to compare Pd hydride formation ability in PdZn/Al_2O_3 and Pd/Al_2O_3 (Figure S1, Online Supplementary Materials). The H_2-TPD profile of Pd/Al_2O_3 displays a desorption peak at 75–90 °C with a maximum at 83 °C characteristic of PdH_x decomposition.[26,28,33] In contrast, no signal was observed in the TPD pattern of the PdZn/Al_2O_3 catalyst reduced at 150 and 400 °C. This observation provides evidence of PdZn solid-state alloy formation even after reduction at 150 °C, in agreement with XPS and XRD data.

Thus, XPS, XRD and H_2-TPD results clearly indicate the formation of solid-state PdZn alloy after reduction at 150–300 °C and its transformation to IMCs as the reduction temperature increases to 350–400 °C. To reveal the effect of this transformation on the catalytic performance in alkyne hydrogenation, the synthesized catalysts were studied in the liquid-phase hydrogenation of diphenylacetylene. Figure 4 shows the kinetic profiles of hydrogen uptake for Pd/Al_2O_3 and PdZn/Al_2O_3 samples reduced at different temperatures. The PdZn/Al_2O_3 catalyst reduced at 200 °C exhibited a distinctly different kinetic behavior, as compared to that of the parent Pd sample. The kinetic profile of PdZn/Al_2O_3 catalyst exhibits pronounced downward bending after the uptake of 1 equiv. of H_2. A comparison of TOF_1 (alkyne to alkene hydrogenation) and TOF_2 (alkene to alkane hydrogenation) values shows that TOF_1 for PdZn/Al_2O_3 decreases by a factor of 4, while TOF_2 decreases by a factor of ~17 in comparison with that of the monometallic Pd/Al_2O_3 (see Table S1 in Online Supplementary Materials). As a result, the TOF_1/TOF_2 ratio (so-called kinetic selectivity) increases by a factor of 4: from 9.61 for Pd/Al_2O_3 to ~38 for PdZn/Al_2O_3. Taking into account H_2-TPD data, we can suggest that the lower TOF_2 value for PdZn/Al_2O_3 catalysts originates from the disappearance of a PdH_x hydride

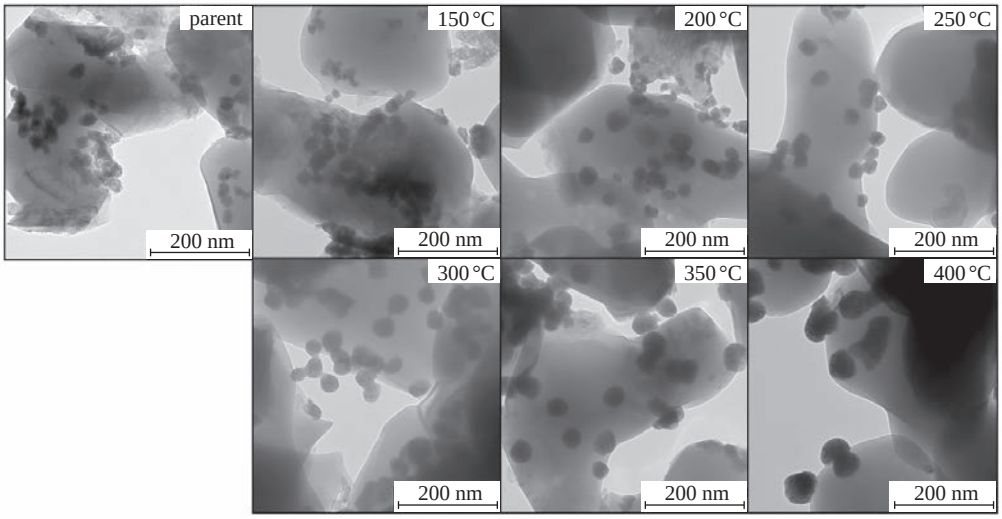

Figure 3 TEM images of parent PdZn/α-Al_2O_3 catalysts and the catalysts reduced at 150–400 °C.

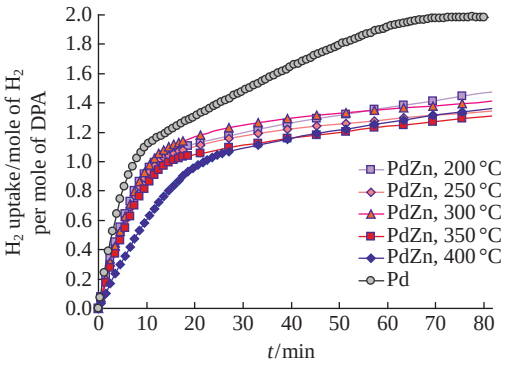

Figure 4 Effect of reduction temperature on the hydrogen uptake for Pd/Al_2O_3 and $PdZn/Al_2O_3$ catalysts in the liquid-phase hydrogenation of diphenylacetylene.

phase due to PdZn alloy formation. The observed change of the general reaction kinetics on the $PdZn/Al_2O_3$ catalyst is of considerable practical interest since it allows one to effectively control the course of the reaction and to stop the hydrogenation after the complete alkyne conversion into olefin.

It is important to note the identity of catalytic performances of $PdZn/Al_2O_3$ samples reduced at 200–400 °C. Only a slight decrease in the overall catalytic activity was observed, which is probably attributed to the enlargement and agglomeration of bimetallic nanoparticles under reduction conditions in accordance with TEM data (Figure 3). The particle size of PdZn IMCs increases from 17 (for PdZn sample reduced at 150 °C) to ~57 nm (after 400 °C treatment). An increase in the reduction temperature also does not lead to appreciable changes in the selectivity of the process. At a 90% alkyne conversion, selectivity of alkene formation for Pd/Al_2O_3 is about 91% while for $PdZn/Al_2O_3$ this parameter is ~92–94% (Table S1). This result clearly indicates that the PdZn solid-state alloy–PdZn intermetallic compound transformation does not exert a significant effect on the catalytic performance.

Thus, a comparison of the catalytic data with XRD, XPS, and H_2 TPD results suggests that the main reason for the change in the overall kinetics of hydrogenation on PdZn catalysts compared to monometallic Pd results mostly from the suppression of a PdH phase due to PdZn substitutional alloy formation, whereas the PdZn solid-state alloy–PdZn IMCs transformation only slightly affects catalytic characteristics.

We are grateful to the Department of Structural Studies of the N. D. Zelinsky Institute of Organic Chemistry, Russian Academy of Sciences for the characterization of the catalysts by electron microscopy.

This study was supported by the Russian Foundation for Basic Research (project no. 16-29-10788).

Online Supplementary Materials

Supplementary data associated with this article can be found in the online version at doi: 10.1016/j.mencom.2018.03.014.

References

1 D. B. Eremin and V. P. Ananikov, *Coord. Chem. Rev.*, 2017, **346**, 2.
2 V. P. Ananikov, K. I. Galkin, M. P. Egorov, A. M. Sakharov, S. G. Zlotin, E. A. Redina, V. I. Isaeva, L. M. Kustov, M. L. Gening and N. E. Nifantiev, *Mendeleev Commun.*, 2016, **26**, 365.
3 V. P. Ananikov, D. B. Eremin, S. A. Yakukhnov, A. D. Dilman, V. V. Levin, M. P. Egorov, S. S. Karlov, L. M. Kustov, A. L. Tarasov, A. A. Greish, A. A. Shesterkina, A. M. Sakharov, Z. N. Nysenko, A. B. Sheremetev, A. Yu. Stakheev, I. S. Mashkovsky, A. Yu. Sukhorukov, S. L. Ioffe, A. O. Terent'ev, V. A. Vil', Yu. V. Tomilov, R. A. Novikov, S. G. Zlotin, A. S. Kucherenko, N. E. Ustyuzhanina, V. B. Krylov, Yu. E. Tsvetkov, M. L. Gening and N. E. Nifantiev, *Mendeleev Commun.*, 2017, **27**, 425.
4 A. V. Nartova, L. M. Kovtunova, Yu. V. Larichev, A. K. Khudorozhkov, A. N. Bobrovskaya, G. V. Shterk and V. I. Bukhtiyarov, *Mendeleev Commun.*, 2017, **27**, 70.
5 P. V. Markov, G. O. Bragina, A. V. Rassolov, I. S. Mashkovsky, G. N. Baeva, O. P. Tkachenko, I. A. Yakushev, M. N. Vargaftik and A. Yu. Stakheev, *Mendeleev Commun.*, 2016, **26**, 494.
6 P. V. Markov, G. O. Bragina, A. V. Rassolov, G. N. Baeva, I. S. Mashkovsky, V. Yu. Murzin, Ya. V. Zubavichus and A. Yu. Stakheev, *Mendeleev Commun.*, 2016, **26**, 502.
7 Y. Yan, J. S. Du, K. D. Gilroy, D. Yang, Y. Xia and H. Zhang, *Adv. Mater.*, 2017, **29**, 1605997.
8 M. Krajči and J. Hafner, *ChemCatChem*, 2016, **8**, 34.
9 S. Furukawa and T. Komatsu, *ACS Catal.*, 2017, **7**, 735.
10 K. Föttinger, *Catalysis*, 2013, **25**, 77.
11 M. Armbrüster, M. Behrens, K. Föttinger, M. Friedrich, É. Gaudry, S. K. Matam and H. R. Sharma, *Cat. Rev. Sci. Eng.*, 2013, **55**, 289.
12 I. S. Mashkovsky, P. V. Markov, G. O. Bragina, G. N. Baeva, A. V. Bukhtiyarov, I. P. Prosvirin, V. I. Bukhtiyarov and A. Yu. Stakheev, *Kinet. Catal.*, 2017, **58**, 471 (*Kinet. Katal.*, 2017, **58**, 499).
13 H. Zhou, X. Yang, L. Li, X. Liu, Y. Huang, X. Pan, A. Wang, J. Li and T. Zhang, *ACS Catal.*, 2016, **6**, 1054.
14 N. T. Mai, T. T. Thuy, D. M. Mott and S. Maenosono, *CrystEngComm*, 2013, **15**, 6606.
15 H. H. Holzapfel, A. Wolfbeisser, C. Rameshan, C. Weilach and G. Rupprechter, *Top. Catal.*, 2014, **57**, 1218.
16 H. Bahruji, M. Bowker, G. Hutchings, N. Dimitratos, P. Wells, E. Gibson, W. Jones, C. Brookes, D. Morgan and G. Lalev, *J. Catal.*, 2016, **343**, 133.
17 J. A. Rodriguez, *J. Phys. Chem.*, 1994, **98**, 5758.
18 N. Iwasa, S. Masuda, N. Ogawa and N. Takezawa, *Appl. Catal., A*, 1995, **125**, 145.
19 A. Baylet, P. Marécot, D. Duprez, P. Castellazzi, G. Groppi and P. Forzatti, *Phys. Chem. Chem. Phys.*, 2011, **13**, 4607.
20 L. Znaidi, T. Touam, D. Vrel, N. Souded, S. Ben Yahia, O. Brinza, A. Fischer and A. Boudrioua, *Coatings*, 2013, **3**, 126.
21 M. J. Akhtar, M. Ahamed, S. Kumar, M. A. M. Khan, J. Ahmad and S. A. Alrokayan, *Int. J. Nanomedicine*, 2012, **7**, 845.
22 H. Bahruji, M. Bowker, W. Jones, J. Hayward, J. Ruiz Esquius, D. J. Morgan and G. J. Hutchings, *Faraday Discuss.*, 2017, **197**, 309.
23 P. S. da Silva, J. M. Maciel, K. Wohnrath, A. Spinelli and J. R. Garcia, in *Modern Surface Engineering Treatments*, ed. M. Aliofkhazraei, InTech, 2013, ch. 9, pp. 209–230.
24 A. A. Veligzhanin, Ya. V. Zubavichus, N. Yu. Kozitsyna, V. Yu. Murzin, E. V. Khramov and A. A. Chernyshov, *J. Surf. Invest. X-Ray Synchrotron Neutron Tech.*, 2013, **7**, 422 (*Poverkhnost. Rentgenovskie, Sinkhrotronnye i Neitronnye Issledovaniya*, 2013, **5**, 26).
25 W. Stadlmayr, C. Rameshan, C. Weilach, H. Lorenz, M. Hävecker, R. Blume, T. Rocha, D. Teschner, A. Knop-Gericke, D. Zemlyanov, S. Penner, R. Schlögl, G. Rupprechter, B. Klötzer and N. Memmel, *J. Phys. Chem. C*, 2010, **114**, 10850.
26 T. Komatsu, K. Inaba, T. Uezono, A. Onda and T. Yashima, *Appl. Catal., A*, 2003, **251**, 315.
27 N. Iwasa, M. Yoshikawa, W. Nomura and M. Arai, *Appl. Catal., A*, 2005, **292**, 215.
28 H. Arnold, F. Döbert and J. Gaube, in *Handbook of Heterogeneous Catalysis*, eds. G. Ertl, H. Knözinger, F. Schüth and J. Weitkamp, Wiley-VCH, Weinheim, 2008, pp. 3266–3283.
29 W. Palczewska, *Adv. Catal.*, 1975, **24**, 245.
30 S. A. Nikolaev, L. N. Zanaveskin, V. V. Smirnov, V. A. Averyanov and K. L. Zanaveskin, *Russ. Chem. Rev.*, 2009, **78**, 231 (*Usp. Khim.*, 2009, **78**, 248).
31 P. V. Markov, G. O. Bragina, G. N. Baeva, O. P. Tkachenko, I. S. Mashkovskii, I. A. Yakushev, M. N. Vargaftik and A. Yu. Stakheev, *Kinet. Catal.*, 2016, **57**, 617 (*Kinet. Katal.*, 2016, **57**, 621).
32 M. Armbruster, M. Behrens, F. Cinquini, K. Fottinger, Yu. Grin, A. Haghofer, B. Klotzer, A. Knop-Gericke, H. Lorenz, A. Ota, S. Penner, J. Prinz, C. Rameshan, Z. Revay, D. Rosenthal, G. Rupprechter, Ph. Sautet, R. Schlögl, L. Shao, L. Szentmiklósi, D. Teschner, D. Torres, R. Wagner, R. Widmer and G. Wowsnick, *ChemCatChem*, 2012, **4**, 1048.
33 A. Borodzinski and G. C. Bond, *Catal. Rev.*, 2006, **48**, 91.

Received: 21st July 2017; Com. 17/5313